A short review of vapour droplet dispersion models used in CFD to study the airborne spread of COVID19

Syed Mehade Hussain [a], Saurav Goel [a,b,c,*], Chennakesava Kadapa [d], Elsa Aristodemou [a]

[a] School of Engineering, London South Bank University, London SE10 AA, UK
[b] University of Petroleum and Energy Studies, Dehradun 248007, India
[c] Indian Institute of Technology Guwahati, Guwahati 781039, India
[d] School of Engineering, University of Bolton, Bolton BL3 5AB, UK

A B S T R A C T

The use of computational fluid dynamics (CFD) to simulate the spread of COVID19 and many other airborne diseases, especially in an indoor environment needs accurate understanding of dispersion models. Modelling the transport/dispersion of vapour droplets within the atmosphere is a complex problem, as it involves the motion of more than one phase, as well as the interphase interactions between the phases. This paper reviews the current canon of research on dispersion modelling of vapour droplets by looking at three specific aspects: (i) physical definition/specification of the initial droplet size distribution; (ii) physics of evaporation/condensation models and (iii) transport equations (with molecular/turbulent dispersion models) to describe the movement of the vapour droplets as they propagate through the air. This review found that the state of modelling implements a wide range of models which shows variances in results thus leading to a state where it is difficult to know which model is most accurate. The authors suggest that further studies in this direction should focus on developing a principle set of equations by benchmarking the previously developed models to establish model uncertainty of the previously developed models with reference to a fixed theoretical model and be compared under identical conditions. However, it must be noted that due to the complex nature of microdroplet evaporation and dispersion coupled with the unpredictable way droplet size distributions are produced, current experimental methodologies that are available to validate such simulations, such as particle image velocimetry, are still not robust enough to provide detailed data to verify minute aspects of the simulations.
Copyright © 2022 Elsevier Ltd. All rights reserved.
Selection and peer-review under responsibility of the scientific committee of the Innovative Technologies in Mechanical Engineering-2021.

1. Introduction

Since the outbreak of SARS-CoV-2 also known as COVID-19 four significant variants of the virus (alpha, beta, gamma, & delta) [1] have been identified that are a cause for concern along with six others that are of interest and are being monitored [2]. The current situation of the COVID-19 pandemic is still ever-evolving and to date three countries are bearing the worst of the brunt: United States (48.5 million cases & 791,000+ deaths), India (34.5 million cases & 465,000+ deaths), and Brazil 22 million cases & 612,000+ deaths) [3].

Global pandemics are slowly becoming increasingly frequent as studies have catalogued the emergence of more than 335 infectious diseases between 1940 and 2004 and in the 21st century alone there has been seven pandemics, including SARS (2002), the Avian Flu (2003), the Swine Flu (2009), MERS (2012), Ebola (2014), Zika (2015), and of course COVID-19 (2019) [4]. In preparation to deal with a future pandemic, although work on vaccine development and improved design of air filter has accelerated, but an improved understanding is required by modelling the mechanics of airborne spread of the virus as an immediate measure to develop informed policies and procedures [5].

It has been recognised that environments in which the spread can accelerate are indoor public spaces, due to insufficient air circulation which intensifies the accumulation of virus within a confined space leading up to inhaling higher concentration of virus

* Corresponding author at: School of Engineering, London South Bank University, London SE10 AA, UK.
  E-mail address: GOELS@Lsbu.ac.uk (S. Goel).

laden media. Within indoor public spaces, schools and office spaces are most vulnerable places to cause accelerated airborne viral transmission [6].

To understand how the spread of such viruses can occur, CFD simulations of respiratory events needs to incorporate elements such as airflow patterns (laminar or turbulent conditions), varying ambient conditions (temperature, humidity), phases involved (gas-liquid-solid) and interphase interactions. For the dispersion of viruses such as COVID-19, within the indoor environment, the effects of breathing, speaking, coughing, and sneezing are of paramount importance to assess the impact on the spread of the virus, as they all eject a cloud of saliva droplets of different sizes which can transport pathogens across an environment.

CFD simulations of coughing, sneezing, speaking, and breathing can provide detailed spatial and temporal information of the virus concentration and status and hence assist in the development of mitigation strategies. Coughing and sneezing tend to be short and intense events where roughly 3,500 and 40,000 droplets are produced in a single event, respectively, but speaking and breathing tend to produce a lower concentration but are inherently longer or even sustained events. Droplets larger than 60 μm tend not to evaporate completely and settle on a surface, but smaller droplets under this size can evaporate at a rapid rate and become suspended in the local atmosphere as droplet nuclei [7]. It is these microdroplets that can potentially carry large numbers of virus but can remain small enough and airborne to be inhaled into the respiratory tract [7].

Any respiratory action modelled in CFD must be considered as a multiphase flow problem involving transport of liquid droplets of saliva (discrete secondary phase), interspersed in a gas cloud continuum (primary phase). Both the discrete and continuum phase have different governing equations but can be combined together through the use of the Eulerian-Lagrangian framework. The Eulerian component models the continuum whilst the Lagrangian component models the discrete liquid particles, and this framework is used exclusively in all of the current RANS-based models. The governing equations for the continuum (gas phase) treats turbulent flow with well-established turbulence models and there have been many studies benchmarking their performances. However, the modelling equations predicting the fate of the liquid droplets have not had the same development, as the physical processes (evaporation and heat transfer) and their associated parameters are not always incorporated, leading to inaccurate predictions.

This review examines the current state of CFD modelling studies of multiphase propagation of discrete liquid droplets within a gas cloud, specifically in three main aspects of modelling (i) the initial droplet size distribution model, (ii) the evaporation model, and (iii) the transport/dispersion model. The review then discusses the current limitations of these models and offer suggestions to direct the future work to make the most of the available models. The last review on dispersion of viruses in indoor spaces was carried out by Ai & Melikov (2018) [8] in 2018 in which important factors of risk of cross-infection, the thermo-fluid boundary conditions of thermal manikins and research techniques and evaluation methods were given special attention. They concluded that further attention should be paid to the ventilation parameter as the direction of the indoor flow pattern is crucial, and also that the minimum social distance to reduce risk of infection should only be up to 1.5 m. Interestingly, there have been several studies since, such as Vuorinen et al (2020) [6], Pendar & Pascoa (2020) [9], and L. Bourouiba (2020) [10] that have suggested distances of over 4 m being a more appropriate distance, particularly in the aftermath of the COVID-19 pandemic outbreak. The review of Ai & Melikov concluded that strong digitalisation tools are required with robust instrumentation to experimentally track aerosols for improved modelling and simulations by obtaining high-temporal-resolution experimental data on airborne transmission.

2. Definition of source: Geometry and droplet size distribution

The boundary conditions of a simulation can be immensely crucial to the accuracy of its predictions. Small changes in ejection velocities or angles can have large effects on the simulation, and in some cases small changes in the shape of the mouth during sneezing can change the dispersion pattern and distance by up to 50% of the original spread [9]. One of the most difficult conditions to set up is the size distribution of the droplets expelled at source.

Considering the ejection of liquid droplets due to breathing, speaking, coughing, and sneezing, the geometry of a person's mouth needs to be specified. As each person has unique characteristics, certain assumptions need to be made. Furthermore, as previously mentioned, coughing and sneezing create different droplet size distributions. Han et al (2013) [11] observed two types of distribution in the size of droplets and found that the average geometric diameter of a sneeze was 386.2 μm for unimodal distribution and 74.4 μm for bimodal distribution. Conversely, the droplet distribution for a cough was found to be multimodal in a study carried out by Yan et al (2007) [12] where the average droplet diameter was 8.35 μm and the distribution showed three peaks at 1, 2, and 8 μm. This would indicate that despite the large number of droplets from a sneeze in comparison to a cough, the majority of the droplets are vastly larger in diameter and would therefore settle fairly quickly. However, it should be noted that larger droplets may travel much farther out before settling due to the initial velocities which can be in the region of 30 to 100 ms^{-1} in contrast to an average of 11.7 ms^{-1} for coughing. The unpredictive way the size and number of droplets are distributed in a cough plume from experimental data is highly complex and every repetition of experiment can produce vastly different results even from the same subject. Therefore, a common approach to represent the ejected droplets is to use a particle density functions (PDFs).

Liu et al (2021) [13] used the Pareto PDF to model 61650 droplets ranging from 1 to 1000 μm, in an LES-based study, and their results showed good agreement with the theoretical prediction. However, in Balachandar et al (2020) [14], using data from Duguid (1946) [15], they indicated that the Pareto distribution, as shown in Fig. 1, was only valid for droplets between 50 to 130 μm in diameter. They also found that a log normal distribution would be a better fit for droplets under 50 μm, which suggests that the number of droplets under 50 μm may have been overinflated.

Dbouk and Drikakis (2020) [16] used the Rosin-Rammler PDF in characterising the droplet size distribution (reference for this?) as shown in Fig. 2. The original Rosin-Rammler equation [17] is stated as:

$$Y = 1 - exp\left(\frac{-x}{x_0}\right)^n \qquad (1)$$

where (Y) is the cumulative fraction of material by weight less than size (x); (n) is the constant describing the material uniformity – also known as the uniformity constant, and (x_0) is the characteristic particle size, defined at which 63.2% of the particles by weight are smaller [18]. A very similar equation in used in the ANSYS code which is expressed as:

$$Y_d = e^{-\left(\frac{d}{\bar{d}}\right)^n} \qquad (2)$$

where (d) is the diameter of the droplet, ($\bar{d}$) is the size constant (or the 'mean diameter'), and (n) is the size distribution parameter (or the 'spread parameter'). Xie et al (2009) [19] attempted to improve the modelling of the size distribution near the origin of ejection and produced the following equation:

$$f = \frac{n}{\bar{d_p}} \left(\frac{d_p}{\bar{d_p}}\right)^{n-1} e^{-\left(\frac{d}{\bar{d_p}}\right)^n}, n = 8, \bar{d_p} = 80 \ \mu m \qquad (3)$$

This PDF is also well-established to produce an accurate image of distribution in the case of water-based droplets in a gas cloud.

The use of the Rosin-Rammler PDF is in conjunction with a larger effort of Dbouk and Drikakis to create a better model for discrete liquid droplet evaporation but it is not explicitly part of the model which will be discussed further on. The model is used in other studies carried out by Dbouk and Drikakis (2020 [20] & 2021 [21]) and is even implemented in studies such as Wu et al (2021) [22], Ge et al (2021) [23], and Chillón et al (2021) [24].

A study by Zhang et al (2020) [25] found that droplets could be classed into two main groups: (a) fine droplets which are assumed to be all spherical, and uniformly diameter droplets of 5 μm, (b) coarser droplets which are modelled using the Rosin-Rammler PDF; in this case, the sizes of the coarser droplets are grouped into eight groups rather than a continuous function - to save computational costs.

In the study of Zhang et al. [25], it was also assumed that velocities of the finer droplets are similar to that of the gas cloud, whilst the coarser droplets are slower, resulting in initial velocities of 10 ms^{-1} and 4.2 ms^{-1} for the fine and coarse droplets, respectively. Their study corroborated well with the experimental data; however, they found simplifications in grouping the size distribution of the droplets and representing them as weighted number of droplets rather than a continuous function had a negative effect on the accuracy, although it was computationally faster. They also found that the evaporation model could be further improved by implementing a user-defined function (UDF) where the forced convection and latent heat modelling could be accounted for as well (to be discussed further in section 3). Another study by Biswas et al (2021) [26] carried out simulations of cough droplet propagation within an elevator very similar to Dbouk and Drikakis (2021) [21] but with different boundary conditions for instance, Dbouk and Drikakis (2020) [21] had eight small 3 cm slits running around the perimeter of the top and bottom of the elevator cabin (top four were inlets, and bottom four were outlets) and a small air purification unit placed behind the subject's head on the cabin wall at approximately 1.9 m. Biswas et al (2021) [26] implemented a sin-
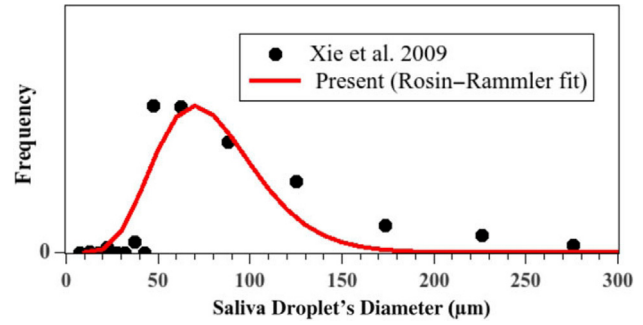

Fig. 2. Rosin-Rammler distribution function corrected by Xie et al (2009) [19] reproduced by Dbouk and Drikakis (2020) [16].

gle circular inlet above the subject and two outlets at the bottom of the cabin running the depth of the cabin. Most interestingly, although they too use the Rosin-Rammler distribution for droplet size, the number of droplets was severely restricted to just over 1000 droplets, which can be considered as little under a third of the normal mount for a cough, however, the reason the reduced amount is unclear. A study by Ge et al (2021) [23] looking at the effects of a variable inlet area to represent a moving mouth, used the Rosin-Rammler distribution as well, however, the distribution graph, shows the peak density of droplet diameter to be just over 20 μm whereas the PDF by Xie et al (2009) [19] the bell curve is much wider with the peak droplet diameter indicated at around 70 μm.

Mirzaie et al (2021) [27] explored droplet dispersion in a classroom environment. In their discrete phase model, they opted for a uniform distribution of droplet sizes of six groups ranging from 0.15 μm to 150 μm in diameter and over 10,800 droplets being released in one 0.75 s long event, far more than is normal. Furthermore, all droplets were assumed to with the same velocity of 10ms^{-1}. Zhang et al (2019) [28] carried out an LES-based study of droplet distribution in air-conditioned rooms and used a similar approach like Mirzaie et al (2021) [27] where droplet sizes were classed into 5 groups (1 μm, 10 μm, 20 μm, 50 μm, and 100 μm) and each group set to release a total of 880 droplets per cough event.
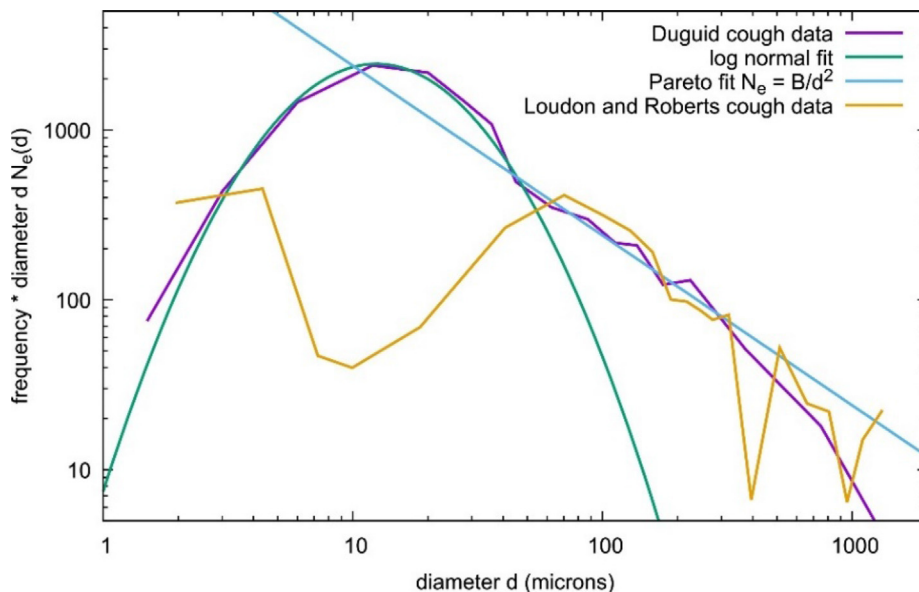

Fig. 1. Droplet distribution data against various distribution functions, Balachandar et al (2020) [14].

3. Evaporation modelling

To accurately model the evaporation of a liquid droplet is an immensely complex problem and the simple equations of heat transfer are not accurate enough due to the influence of other environmental factors that need to be considered, and more often than not, certain approximations are made to simplify the problem. Typically, modelling the evaporation/condensation of liquid droplets requires (i) the composition of the liquid droplet – whether single component or multicomponent droplets are considered; the latent heat of vaporisation of the liquid phases – associated with the phase changes; saturation pressures and temperatures; the temperature and humidity of the environment; liquid droplet temperature and dimensions; the Sherwood number and the molecular diffusivity of the gas.

Approximations may need to be reconsidered when simulations do not match the experimental data, despite the fact that boundary conditions may be the same. Revisiting the physical models and re-assessing the physical processes associated with the development of liquid droplets and their evaporation/dissipation/settling becomes a necessity. Historically, there has been a competition model improvement and model approximation – the latter being implemented due to limiting resources and technology; however, in recent years the model improvement approach has become the favoured option.

A perfect example of this is the work of Dbouk and Drikakis (2020) [16], where they found that the Ranz-Marshall model [29 30] defined the Nusselt and Sherwood numbers as functions of the Reynolds, Prandtl, and Schmidt numbers. However, the equations concerned are valid for steady-state heat and mass transfer rates of spherical particles made of one material only, and that many studies before theirs were incorrectly using the model in transient simulations. They developed new correlations for the Nusselt and Sherwood number as functions of the Reynolds, Prandtl, and Schmidt numbers as well as including fluid and thermodynamic properties of the SARS-CoV-2 virus. Their results found that the relative difference between the standard Ranz-Marshall (Old Theory) model and the new approach (New Theory equations) was as high as 600% at the instant of droplet-air impact, shown in Fig. 3, meaning that predictions using the standard model in a transient multi-material study would be severely underestimated, especially at the initial stages of the simulations.

As can be seen from Fig. 3, at later times, the Old Theory and New Theory curves begin to converge i.e., reach the same plateau. Other studies have subsequently adopted the Dbouk and Drikakis' model and implemented it into their own studies, Dbouk & Drikakis go on to use this model in all their subsequent works (Dbouk & Drikakis 2020 [20], and Dbouk & Drikakis 2021) [21], Wu et al (2021) [22] also implemented the Dbouk and Drikakis evaporation model and were able to conclude that the use of an AC unit can transport droplets further than they would with no forced ventilation and the added turbulence allows for droplets to evaporate faster and become inhalable droplet nuclei.

The Dbouk & Drikakis model is by no means ubiquitous in implementation as other studies such as Chillón et al (2021) [24] use the standard Ranz-Marshall model in their study of cough droplet deposition in a calm confined space. They found that droplets smaller than 10 μm were not initially detectable and only became so after almost 2 s into the simulation. They concluded this was caused by the larger droplets evaporating and becoming smaller droplets. However, this may also be an indication of the standard Ranz-Marshall incorrectly modelling transient evaporation rates as Dbouk & Drikakis suggested.

Zhang et al (2019) [28] carried out an LES-based study where vaporisation of droplets was modelled as single component,

meaning the effect of non-volatile content with the droplet was not considered. The evaporation model implemented was the standard Ranz-Marshall model and an experiment was carried out to validate the simulation; however, they found that direct comparison on the data was not possible and for this reason - a dimensionless concentration factor, defined at the following:

$$C(\%) = \frac{\bar{C}(x,t)}{C_0} \tag{4}$$

where $C(x,t)$ is the average concentration of the droplet aerosols at the measuring point (x) and (C_0) is the initial concentration in the nose.

The experiment consisted of three sensors placed at three heights (sensor 1: +400 mm, sensor 2: +200 mm, and sensor 3: −200 mm), all 100 mm in front of the nose where an aerosol mix was released through hoses. An aerosol monitor, which had an accuracy of 0.001 mgm³, was used to measure the concentration which resulted in good agreement with the experimental data, with the maximum difference in concentration between the experimental data and simulation to be 0.03% for sensor 1, 0.19% for sensor 2, and 0.08% for sensor 3. They found that whilst the ventilation rate and air distribution patterns of the environment played a much more prominent role in the evaporation of droplets than the temperature gradients and humidity. Increasing the humidity level increased the hygroscopic effect which in turn, increases the number of deposited droplet aerosols.

Biswas et al (2021) [26] implemented the standard Ranz-Marshall model by considering the droplets as a mixture of salt and liquid water (99% water and 1% NaCl by weight), meaning that the model would not be able to account for the change in water vapour pressure as the droplet reaches the end of the evaporation process and possibly show the droplet completing evaporation earlier than it should.

Ge et al (2021) [23] implemented the Ranz-Marshall model but only to define the Nusselt number based on the Prandtl number. However, the Sherwood number, which would normally also be defined by the Ranz-Marshall model, is instead defined using a separate equation; the authors also consider the Schmidt number much like Dbouk & Drikakis [16 20 21]. They found that most of the evaporation process takes place within 0.5 s of the cough event where evaporation is at its highest rate and then as the gas cloud cools, the evaporation rate is decreased.

Liu et al (2021) [13] expresses, within the evaporation equation of small droplets, the evaporation coefficient as several factors of the Stokes value, which is based on the Reynolds number, as well as the Spalding mass number. The heat transfer model incorporated the Prandtl and Reynolds number to account for the Nusselt number, and then as the droplet approaches the end of evaporation another equation is used to calculate the final diameter using the D^2 law.

Zhang et al (2020) [25] expressed the composition of their droplets as water, glycerine, and sodium chloride with a mass ratio of $100 : 76 : 12$ and describes the evaporation model using the Sherwood number and without the mention of the Nusselt number. They found that the evaporation model could be further improved by using a user-defined function which could account for forced convection conditions as they had in their simulations and experiments as well as latent heat modelling within the same model.

Mirzaie et al (2021) [27] follow a similar approach to Zhang et al (2019) [28] in defining their evaporation model; however, they opt out of using the Ranz-Marshall model and instead define the Nusselt number independently, using Reynolds and Schmidt number within their equation. Furthermore, they also implemented another heat transfer model accounting for convective
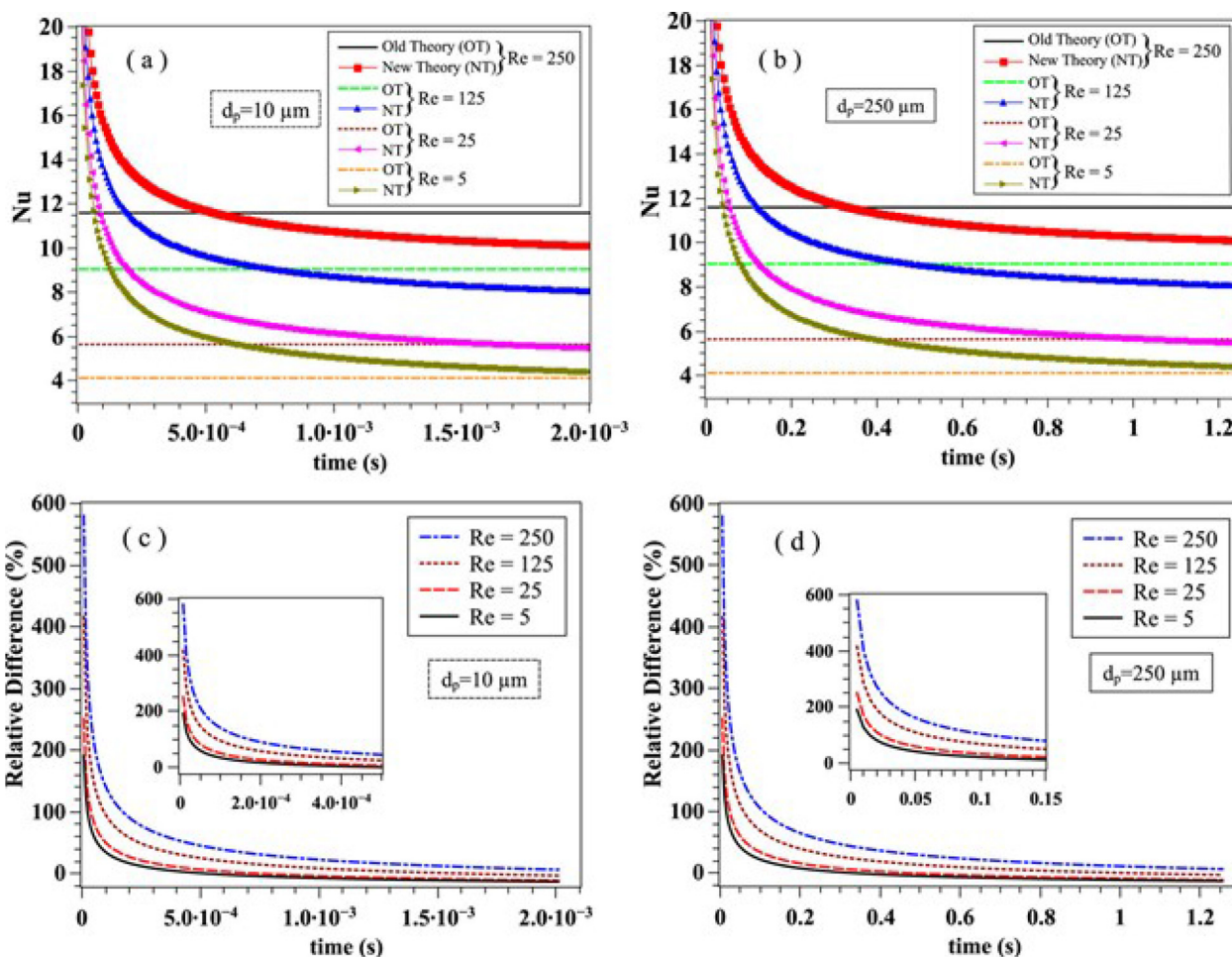
Fig. 3. Transient Nusselt correlation compared with steady-state Ranz-Marshall correlation at different Reynolds numbers and diameters, Dbouk and Drikakis (2020) [20].

and latent heat transfer between the droplet and continuum phase. The research approach of this study was unique in that one of the assumptions made prior to modelling was that the droplet sizes defined that would be released were all evaporated droplets and so the focus of the study was more so on the dispersion patterns within the classroom environment they had selected. Another point of interest is that the ejected droplets were stated to have an initial temperature of 37 °C, which could be contested as implausible as this would require the human body to be at a slightly higher temperature due to the laws of thermodynamics; the usual temperature of ejected droplets is usually a 32 °C – 35 °C as indicated by Dbouk and Drikakis (2020) [16] and Walker et al (2021) [31].

4. Dispersion modelling

In tracking the dispersion of discrete liquid droplets, the Eulerian-Lagrangian method can be comfortably considered the most popular method to use. The continuum phase (air) was modelled using the Eulerian equations, whilst the discrete phase (liquid droplets) was modelled using the Lagrangian approach. The studies reviewed here have all used the Eulerian-Lagrangian method, however, the focus of this review is more so on the models that are implemented to describe drag, liquid particle break-up, and coalescence. These models much like the evaporation models have varying methods and must be subject to the same scrutiny as the evaporation models to ascertain which models are most appropriate.

Chillón et al (2020) [24] used the Schiller-Naumann correlation to obtain the drag coefficients of droplets and interpolate the drag for other droplets as they found resolving the drag coefficients for all droplets would be impractical. They also used the two-way coupled Taylor analogy break-up (TAB) model to account for the interactions between the airflow and the droplets which represents the distortion of a droplet in a spring mass damping system. They found that the droplet cloud dispersed in a V-shape from the mouth origin and that within the gas cloud would lead the larger droplets to tend towards the bottom of the cloud whilst the lighter, smaller droplets were usually at the top and farthest away. They tested three initial ejection velocities and found that the bottom of the gas cloud increased in volume at lower velocities.

Biswas et al (2021) [26] carried out a study using the open source CFD platform OpenFOAM and defined the dispersion model using two user-defined functions which included an equation to describe the motion of a droplet and an equation for the lift force. They also implemented equations to describe the drag coefficient and an energy-conservation equation which may have acted as a break-up, but no such models were explicitly defined. They found that the absence of ventilation meant that a significantly large percentage of droplets remained suspended in their elevator environment; by introducing forced ventilation a maximum of just over 29% remained suspended and in other cases all the droplets were either extracted or settled; this study indicated the importance of ventilation.

Ge et al (2021) [23] implemented two drag coefficient equations with boundaries defined using the Reynolds number, with

two separate values for Reynolds numbers equal and above 1000 and another for below 1000. They also used the Kelvin-Helmholtz Rayleigh-Taylor break-up model, and the O-Rourke model was used to describe collision and coalescence between droplets. They found that, in three different temperature scenarios (295 K, 290 K, and 285 K), there is no evident difference in droplet penetration during the first half-second ($t = 0.5$ to 1) after the cough had finished ($t = 0.5$) due to the droplets remaining inside the gas cloud. After this, however, the room temperature will gradually exert an influence on the temperature profile of the gas cloud and dispersion will begin to vary. They also found that in lower temperatures there was more droplet penetration implying vapour density having an effect on the propagation.

Zhang et al (2020) [25] defined drag in their dispersion model by simply stating the drag law was spherical, with no additional details. Their study did not specify a break-up model nor a coalescence model which implies the study was more inclined to focus on the evaporation aspect of the simulation. Nevertheless, their study found that whilst good ventilation and a high air change per hour value can significantly reduce the likelihood of inhalation of droplet aerosols, the influence of a recirculating air conditioning unit increased droplet aerosol inhalation by 32% at the highest speed.

Zhang et al (2019) [28] expressed the particle momentum equation using Stoke's drag modification function for large particle Reynolds number as well as the Cunningham slip correction factor. They found that the initial velocities of respiratory actions directly affected the distribution of droplet aerosols and that aerosols with initial diameters < 20 μm all suspended in the atmosphere at a similar height. Crucially, they also observed that droplet aerosols with initial diameters of 100 μm tended to become suspended around the breathing zone, which may result in easier human exposure.

Mirzaie et al (2021) [27] defines the equation of motion using the Saffman lift force, the Brownian force, and a coefficient of drag which was defined using the Cunningham coefficient. This study was solely focused on dispersion as all particles were considered evaporated and so no evaporation model was implemented. They found that the particles from a cough would initially rise in a single collated plume from the coughing subject but become dispersed as the droplets interacted with air flow pattern of the ventilation inlet. The extraction of the dispersed droplets was then dependent on the velocity of the inlet air and found inlet velocities as low as $3~\text{ms}^{-1}$, the slowest of the three velocities, to be severely inadequate as it failed to extract a significant amount of particles whereas the higher velocities ($5~\text{ms}^{-1}\,\&\,7~\text{ms}^{-1}$) extracted almost all particles in under 60 s.

Dbouk & Drikakis (2020) [16] used the Weber number to describe the relationship between the carrier fluid inertia forces and the droplet's surface tension forces, and then used the Pilch & Erdman break-up model which is closely tied with the Weber number. They found that droplets in air will fall to the ground in a short amount of time and the range may not exceed 1 m and any remaining droplets that travel further tend not to be at breathing heights for adults. However, at low speeds, which is usually the case, the evaporation rate increases and travel significantly further rendering the 2 m social distancing rule inadequate.

Dbouk & Drikakis (2021) [21] go on to use the same modelling equations in their study looking at dispersion in an elevator. They found that the placement of inlets and outlets heavily influence the dispersion patterns and that introducing an air purifier induced flow circulation and transported the droplet aerosols further and resulted in more mixing of the aerosols which meant they stayed buoyant for longer. They also suggested in such a confined environment, the use of UV light to deactivate the virus may be a more efficient method of elimination.

Wu et al (2021) [22] also implemented the same dispersion model as Dbouk & Drikakis as they did with the evaporation model, however, on this instance they opted to define the drag using an equation which included the Brownian force and Saffman lift force similar to Mirzaie et al (2021). Their findings were mentioned already in the evaporation modelling section of this review.

Liu et al (2021) [13] only defined the dispersion modelling using a theoretical model developed by Balachandar et al (2020) [14] for accurately predicting the number of droplet nuclei that remain airborne for extended periods of time which allows good estimates to be made with the need for full-fledged experiments or simulations. They found good agreement with the model and concluded that dry ambient conditions increase the amount of droplet aerosols by a factor of four and ejected droplets self-sort themselves into large droplets that fall out of the gas cloud quickly, and smaller droplets that fully evaporate and become droplet nuclei.

5. Concluding remarks

The efforts made in the studies reviewed in this paper show that whilst there is popularity with the use of the Rosin-Rammler distribution function, there are still studies that are not implementing this function and using other means of defining the droplet size distribution boundary condition. This means that there is still not a complete consensus on which model is most appropriate for defining the size distribution and more work needs to be carried out to categorically define and establish the accuracy of distribution methods reported in literature.

These studies also represent the current state of discrete liquid particle evaporation modelling and similar to the state of distribution, it can be inferred that there is no consensus on how to model evaporation using continuum approaches. In some studies, such as Mirzaie et al (2021) [27], the evaporation of droplets may not be the focus, yet there are at least five different approaches proposed to model the evaporation process with some proposing same or similar evaporation equations but differing coefficients for various dimensionless numbers and ratios; this may be due to the differences in the boundary conditions and specification of source functions that each study has chosen to implement. The result of this variance is that it becomes incredibly difficult to ascertain if any particular model is accurate, as most studies conclude that the simulation was in good agreement with experimental results to some extent. It is difficult to say which study was more erroneous than another when compared with experiments as no experimental study has been compared to the experiments in real-time and it points to the need of developing improved experimental methods to measure so that the modelling community can swiftly use the experimental data for model validation and verification.

In reviewing the dispersion and evaporation modelling parameters of these studies, it became apparent that more focus is placed on the evaporation modelling aspect of the simulations. This may be for several reasons; it may be because evaporation modelling is least understood while dispersion parameters such as drag, and break-up models have long been understood. However, it could be argued that the state of dispersion modelling is just as varied as evaporation modelling with no single unique author implementing an identical or almost identical dispersion model which would put the variance of dispersion modelling higher than evaporation modelling. The table below, (see Table 1), summarises various methods each study that has been reviewed in this paper, defined their initial droplet size distribution, their evaporation model, and dispersion model.

In examining the table, one inference that becomes apparent is that there is indeed no single set of equations that act as the benchmark for modelling, which can be considered accurate, and the

Table 1
Summary of the models used in the studies reviewed by this paper.

Study	Droplet Size Distribution	Evaporation Modelling	Dispersion Modelling
Biswas et al (2021) [26]	Rosin-Rammler	Ranz-Marshall model (steady-state)	Equation of motion of droplet; lift force; drag coefficient & energy-conservation.
Chillón et al (2021) [24]	Rosin-Rammler	Ranz-Marshall model (steady-state)	Schiller-Naumann correlation; two-way coupled Taylor analogy break-up (TAB) model.
Dbouk & Drikakis (2020) [16]	Rosin-Rammler	Ranz-Marshall model (transient)	Weber no. for drag; Pilch & Erdman break-up model.
Dbouk & Drikakis (2021) [21]	Rosin-Rammler	Ranz-Marshall model (transient)	Weber no. for drag; Pilch & Erdman break-up model.
Ge et al (2021) [23]	Rosin-Rammler	Ranz-Marshall model (steady-state) for Nusselt no. UDF for Sherwood & Schmidt no.	2 drag coefficients ($Re \geq 1000$)&($Re < 1000$). Kelvin-Helmholtz Rayleigh-Taylor break-up model; O-Rourke model for collision & coalescence.
Liu et al (2021) [13]	Pareto	UDF using Stoke's, Reynolds, Spalding mass no., Prandtl, & Nusselt no.	Saffman lift force; Brownian force; Pilch & Erdman break-up model.
Mirzaie et al (2021) [27]	6 groups (0.15, 1, 10, 50, 100, 150 µm) count 1800 each	Ranz-Marshall model (steady-state) for Sherwood no., UDF for Nusselt no.	Saffman lift force; Brownian force; Cunningham coefficient for drag.
Wu et al (2021) [22]	Rosin-Rammler	Ranz-Marshall model (transient)	Saffman lift force; Brownian force;
Zhang et al (2019) [28]	5 groups (1, 10, 20, 50, 100 µm) count 880 each	Ranz-Marshall model (steady-state)	Stoke's drag modification function & Cunningham slip correction factor.
Zhang et al (2020) [25]	Fine droplets: (5 µm @10 ms^{-1}) Coarse droplets: Rosin-Rammler	Nusselt & Sherwood no.	Drag law: Spherical

principle set of equations to use when indoor multiphase discrete liquid evaporation and dispersion is to be modelled. Therefore, it is authors' view that a further systematic study is needed, which will allow a thorough comparison and benchmarking of all the existing models proposed in the literature under identical conditions to fully identify the optimal CFD modelling approach. This new data will serve to make further refinements towards improving the accuracy of multiphase dispersion modelling in indoor environments. Efforts in this direction in other areas of modelling i.e., transferability and benchmarking of the potential function or force-fields used to model carbon-carbon interaction in diamond-like-carbon (DLC) coatings are already happening, so it is no surprise that the field of CFD has reached a point, where transferability of equations and their benchmarking has become a strong need [32 33].

CRediT authorship contribution statement

Syed Mehade Hussain: Conceptualization, Methodology, Investigation, Resources, Data curation, Writing – original draft. **Saurav Goel:** Methodology, Formal analysis, Resources, Writing – review & editing, Supervision, Project administration, Funding acquisition. **Chennakesava Kadapa:** Writing – review & editing, Supervision. **Elsa Aristodemou:** Resources, Writing – review & editing, Supervision.

Declaration of Competing Interest

The authors declare that they have no known competing financial interests or personal relationships that could have appeared to influence the work reported in this paper.

Acknowledgements

References

[1] S. Goel, S. Hawi, G. Goel, V.K. Thakur, A. Agrawal, C. Hoskins, O. Pearce, T. Hussain, H.M. Upadhyaya, G. Cross, A.H. Barber, Resilient and agile engineering solutions to address societal challenges such as coronavirus pandemic, 17 (2020) 100300. https://doi.org/10.1016/j.mtchem.2020.100300.

[2] W.H. Organization, SARS-CoV-2 Variants of Concern and Variants of Interest, (2021). https://www.who.int/en/activities/tracking-SARS-CoV-2-variants/ (accessed June 11, 2021).

[3] Worldometers, COVID Live Update - Worldometer, (2021). https://www.worldometers.info/coronavirus/ (accessed June 11, 2021).

[4] A. Chin, G.L. Simon, P. Anthamatten, K.C. Kelsey, B.R. Crawford, A.J. Weaver, Pandemics and the future of human-landscape interactions 31 (2020) 100256. https://doi.org/10.1016/j.ancene.2020.100256.

[5] A. Shishkin, G. Goel, J. Baronins, J. Ozolins, C. Hoskins, S. Goel, Using circular economy principles to recycle materials in guiding the design of a wet scrubber-reactor for indoor air disinfection from coronavirus and other pathogens, 22 (2021) 101429. https://doi.org/10.1016/j.eti.2021.101429.

[6] V. Vuorinen, M. Aarnio, M. Alava, V. Alopaeus, N. Atanasova, M. Auvinen, N. Balasubramanian, H. Bordbar, P. Erästö, R. Grande, N. Hayward, A. Hellsten, S. Hostikka, J. Hokkanen, O. Kaario, A. Karvinen, I. Kivistö, M. Korhonen, R. Kosonen, J. Kuusela, S. Lestinen, E. Laurila, H.J. Nieminen, P. Peltonen, J. Pokki, A. Puisto, P. Råback, H. Salmenjoki, T. Sironen, M. Österberg, Modelling aerosol transport and virus exposure with numerical simulations in relation to SARS-CoV-2 transmission by inhalation indoors, Saf. Sci. 130 (2020) 104866, https://doi.org/10.1016/j.ssci.2020.104866.

[7] R.R. Netz, Mechanisms of Airborne Infection via Evaporating and Sedimenting Droplets Produced by Speaking, 124 (2020) 7093–7101. https://doi.org/10.1021/acs.jpcb.0c05229.

[8] Z.T. Ai, A.K. Melikov, Airborne spread of expiratory droplet nuclei between the occupants of indoor environments: A review, 28 (2018) 500–524.

[9] M.-R. Pendar, J.C. Páscoa, Numerical modelling of the distribution of virus carrying saliva droplets during sneeze and cough, 32 (2020) 083305. https://doi.org/10.1063/5.0018432.

[10] L. Bourouiba, Turbulent Gas Clouds and Respiratory Pathogen Emissions: Potential Implications for Reducing Transmission of COVID-19, 323 (2020) 1837–1838. https://doi.org/10.1001/jama.2020.4756.

[11] Z.Y. Han, W.G. Weng, Q.Y. Huang, Characterizations of particle size distribution of the droplets exhaled by sneeze 10 (2013) 20130560. https://doi.org/10.1098/rsif.2013.0560.

[12] J. Yan, M. Grantham, J. Pantelic, P.J. Bueno de Mesquita, B. Albert, F. Liu, S. Ehrman, D.K. Milton, E. Consortium, Infectious virus in exhaled breath of symptomatic seasonal influenza cases from a college community, 115 (2018) 1081–1086. https://doi.org/10.1073/pnas.1716561115.

[13] K. Liu, M. Allahyari, J.S. Salinas, N. Zgheib, S. Balachandar, Peering inside a cough or sneeze to explain enhanced airborne transmission under dry weather, 11 (2021) 1–9. https://doi.org/10.1038/s41598-021-89078-7.

[14] S. Balachandar, S. Zaleski, A. Soldati, G. Ahmadi, L. Bourouiba, Host-to-host airborne transmission as a multiphase flow problem for science-based social distance guidelines, 132 (2020) 103439. https://doi.org/10.1016/j.ijmultiphaseflow.2020.103439.

[15] J.P. Duguid, The size and the duration of air-carriage of respiratory droplets and droplet-nuclei, 44 (1946) 471–479. https://doi.org/10.1017/S0022172400019288.

[16] . Dbouk, D. Drikakis, On coughing and airborne droplet transmission to humans, 32 (2020) 053310. https://doi.org/10.1063/5.0011960.

[17] P. Rosin, Laws governing the fineness of powdered coal, 7 (1933) 29–36.

[18] P.A. Vesilind, The Rosin-Rammler particle size distribution, 5 (1980) 275–277. https://doi.org/10.1016/0304-3967(80)90007-4.un.

[19] X. Xie, Y. Li, H. Sun, L. Liu, Exhaled droplets due to talking and coughing, 6 (2009) S703–S714. https://doi.org/10.1098/rsif.2009.0388.focus.

[20] T. Dbouk, D. Drikakis, Weather impact on airborne coronavirus survival, 32 (2020) 093312. https://doi.org/10.1063/5.0024272.

[21] T. Dbouk, D. Drikakis, On airborne virus transmission in elevators and confined spaces, 33 (2021) 011905. https://doi.org/10.1063/5.0038180.

[22] L. Wu, X. Liu, F.Yao, Y. Chen, Numerical study of virus transmission through droplets from sneezing in a cafeteria, 33 (2021) 023311. https://doi.org/10.1063/5.0040803.

[23] H. Ge, L. Chen, C. Xu, X. Cui, Large-eddy simulation of droplet-laden cough jets with a realistic manikin model, (2021) 1420326X211032247. https://doi.org/10.1177/1420326X211032247.

[24] S.A. Chillón, A. Ugarte-Anero, I. Aramendia, U. Fernandez-Gamiz, E. Zulueta, Numerical Modelling of the Spread of Cough Saliva Droplets in a Calm Confined Space, 9 (2021) 574.

[25] B. Zhang, G. Guo, C. Zhu, Z. Ji, C.-H. Lin, Transport and trajectory of cough-induced bimodal aerosol in an air-conditioned space, Indoor Built Environ. 30 (9) (2021) 1546–1567.

[26] R. Biswas, A. Pal, R. Pal, S. Sarkar, A. Mukhopadhyay, Risk Assessment of COVID Infection by Respiratory Droplets from Cough for Various Ventilation Scenarios Inside an Elevator: An OpenFOAM based CFD Analysis, (2021).

[27] M. Mirzaie, E. Lakzian, A. Khan, M.E. Warkiani, O. Mahian, G. Ahmadi, COVID-19 spread in a classroom equipped with partition – A CFD approach, 420 (2021) 126587. https://doi.org/10.1016/j.jhazmat.2021.126587.

[28] Y. Zhang, G. Feng, Y. Bi, Y. Cai, Z. Zhang, G. Cao, Distribution of droplet aerosols generated by mouth coughing and nose breathing in an air-conditioned room, 51 (2019) 101721. https://doi.org/10.1016/j.scs.2019.101721.

[29] W.R. Marshall, W.E. Ranz, Evaporation From Drops—Part I (48) (1952) 141–146.

[30] W.E. Ranz, W.R. Marshall, Evaporation from drops: II. Chem 48 (1952) 173–180.

[31] J.S. Walker, J. Archer, F.K.A. Gregson, S.E.S. Michel, B.R. Bzdek, J.P. Reid, Accurate Representations of the Microphysical Processes Occurring during the Transport of Exhaled Aerosols and Droplets, 7 (2021) 200–209. https://doi.org/10.1021/acscentsci.0c01522.

[32] C. de Tomas, A. Aghajamali, J.L. Jones, D.J. Lim, M.J. López, I. Suarez-Martinez, N.A. Marks, Transferability in interatomic potentials for carbon, 155 (2019) 624–634. https://doi.org/10.1016/j.carbon.2019.07.074.

[33] C. de Tomas, I. Suarez-Martinez, N.A. Marks, Graphitization of amorphous carbons: A comparative study of interatomic potentials, 109 (2016) 681–693. https://doi.org/10.1016/j.carbon.2016.08.024